Frequency variations of quasi-periodic ELF-VLF emissions: A possible new ground-based diagnostic of the outer high-latitude magnetosphere

Jennifer Alford and Mark Engebretson

Augsburg College, Minneapolis, Minnesota

Roger Arnoldy

University of New Hampshire, Durham

Umran Inan

Stanford University, Stanford, California

Abstract. Magnetic pulsations and quasi-periodic (QP) amplitude modulations of ELF-VLF waves at Pc 3-4 frequencies (15-50 mHz) are commonly observed simultaneously in cusp-latitude data. The naturally occurring ELF-VLF emissions are believed to be modulated within the magnetosphere by the compressional component of geomagnetic pulsations formed external to the magnetosphere. We have examined data from South Pole Station ($L \sim 14$) to determine the occurrence and characteristics of QP emissions. On the basis of 14 months of data during 1987 and 1988 we found that QP emissions typically appeared in both the 0.5-1 kHz and 1-2 kHz receiver channels at South Pole Station and occasionally in the 2-4 kHz channel. The QP emission frequency appeared to depend on solar wind parameters and interplanetary magnetic field (IMF) direction, and the months near fall equinox in both 1987 and 1988 showed a significant increase in the percentage of QP emissions only in the lowest-frequency channel. We present a model consistent with these variations in which high-latitude (nonequatorial) magnetic field minima near the magnetopause play a major role, because the field magnitude governs both the frequency of ELF-VLF emissions and the whistler mode propagation cutoffs. Because the field in these regions will be strongly influenced by solar wind and IMF parameters, variations in the frequency of such emissions may be useful in providing ground-based diagnostics of the outer high-latitude magnetosphere.

1. Introduction

A variety of naturally occurring low-frequency radio emissions are observed in the Earth's polar regions. It has often been observed that naturally occurring ELF-VLF radio emissions (~0.5-4 kHz) are modulated quasi-periodically in the range of ~10-50 s [*Helliwell*, 1965; *Carson et al.*, 1965]. Often these quasi-periodic (QP) modulations are observed with simultaneous geomagnetic pulsations of roughly the same ULF frequency. For these simultaneous observations it is generally accepted that the compressional component of the ULF geomagnetic pulsations modulates the ELF-VLF waves through transverse acceleration of the trapped electrons [*Coroniti and Kennel*, 1970; *Haugstad*, 1976; *Sato and Fukunishi*, 1981].

QP events are characterized by a sinusoidal envelope of the ELF-VLF signal amplitude or by repetitive bursts of ELF-VLF noise consisting of discrete elements [*Ho*, 1973]. Quasi-periodically modulated ELF-VLF emissions have been ob-

served at stations ranging in geomagnetic latitude from ~50° to ~80°. Several authors have reported events where simultaneous quasi-periodic ELF-VLF observations have been made at several stations separated by several L shells [*Carson et al.*, 1965; *Morrison et al.*, 1994]. However, the geomagnetic pulsations typically observed during those periods did not show such coherence.

Previous researchers [*Kitamura et al.*, 1969; *Sato and Kokubun*, 1981; *Tixier and Cornilleau-Wehrlin*, 1986] have divided quasi-periodic emissions into two categories. Type 1 events are correlated with magnetic pulsations. Type 2 events are observed without the corresponding magnetic signature or appear to be uncorrelated with the locally observed geomagnetic pulsations. Type 1 events are understood to be caused by geomagnetic pulsations and are easily identified by comparing band-pass ELF-VLF data with magnetometer data. Type 2 events generally show better periodicity, are frequently characterized by rising tone emissions, and are also more frequently observed at lower-latitude stations [*Sato and Kokubun*, 1981]. *Sato and Fukunishi* [1981] show several examples of the different spectral signatures of QP events and note that most daytime type 1 events at auroral zone latitudes are nondispersive (with simultaneous amplitude modulation at all affected frequencies), but a wide variety of modulation envelopes have been observed.

We present in this report observations of a seasonal variation in the occurrence and characteristics of type 1 quasi-periodic emissions at South Pole Station, Antarctica, during a 14-month period during 1987 and 1988. *Sato et al.* [1990] observed a seasonal variation in the occurrence and characteristics of ELF-VLF hiss observed at Syowa and Husafell, conjugate auroral zone stations. They suggested that the variation in ELF-VLF intensity was linked to the scale height of the ionosphere. In their model the duration of sunlight each day at the observation station is the primary control mechanism for the seasonal variation. The seasonal variation they observed was symmetric about the solstices with a maximum in June, whereas we observe a maximum near fall equinox. However, it is important to note that we present observations of quasi-periodic modulation of VLF hiss, rather than just the occurrence and amplitude of VLF hiss, which may partially account for the observed differences. We will present here another possible contributing factor to the seasonal variation which more adequately explains our results.

The source of the ELF-VLF radio emissions for type 1 events is believed to be an instability associated with electrons trapped in the Earth's magnetosphere [*Coroniti and Kennel,* 1970; *Haugstad,* 1976], whereas the geomagnetic pulsations could be caused by a source external to the magnetosphere [*Morrison et al.,* 1994; *Greenstadt and Russell,* 1994]. In such a scenario the geomagnetic pulsations must interact with the local electron population somewhere in the Earth's magnetosphere to produce the observed quasi-periodic emissions. *Sato and Kokubun* [1981] and *Sato and Fukunishi* [1981] suggested an equatorial source region for the quasi-periodic modulation. As an alternative, *Kitamura et al.* [1969], *Morrison et al.* [1994], and *Morrison and Freeman* [1995] have proposed that a nonequatorial source region may contribute to the modulation of the quasi-periodic emissions observed at high latitudes. The seasonal variation in the occurrence and characteristics of QP events presented in this report supports the *Morrison et al.* [1994] claim that ELF-VLF emissions can also be modulated at high latitudes in the outer magnetosphere.

Previous observations from South Pole Station have suggested the importance of quasi-periodic ELF-VLF events in characterizing the interaction between the solar wind and the Earth's magnetosphere [*Lanzerotti et al.,* 1986; *Engebretson et al.,* 1990, 1991; *Morrison et al.,* 1994]. Around local magnetic noon, South Pole Station is located under the nominal position of the magnetospheric cleft-cusp region. *Engebretson et al.* [1990, 1991] showed a convincing relationship between upstream waves and ground-based observations of geomagnetic pulsations and ELF-VLF emissions. Because of this apparent direct link between upstream waves and QP emissions, it is possible that QP emissions might be used as a tool for diagnosing the upstream geospace environment. In this study we suggest using QP emissions also as a ground-based diagnostic for conditions in the high-latitude outer magnetosphere.

2. Instrumentation

ELF-VLF and search coil magnetometer data from South Pole Station (geographic latitude -90°, invariant latitude -74°, local magnetic noon 1530 UT) from September 1987 through October 1988 (data tapes from November and December 1988 were unreadable) were studied to establish trends in the seasonal variations in the occurrence and characteristics of quasi-periodic (QP) ELF-VLF emissions. ELF-VLF data used in this

study are from the Stanford University ELF-VLF receiver, which includes a vertical-loop antenna oriented for maximum sensitivity in the local magnetic north-south direction with five narrowband filter outputs covering the range from 0.5 to 38 kHz. The ELF-VLF band-pass power was sampled once per second for each channel. This study will focus on channels 1-3. These are denoted VLF1 (0.5-1.0 kHz), VLF2 (1.0-2.0 kHz), and VLF3 (2.0-4.0 kHz). Geomagnetic fluctuations in the 0.001 Hz to 0.5 Hz range were also obtained at a rate of one sample per second, using the University of New Hampshire-University of Minnesota search coil magnetometers. These magnetometers measure the time derivative of the magnetic field and are calibrated in nanoteslas per second [*Taylor et al.,* 1975]

3. Case Studies

For each of the two cases below we show magnetic and ELF-VLF pulsation data from South Pole Station as a dynamic spectrogram and a single spectrum and Interplanetary Monitoring Platform (IMP) 8 satellite observations of the interplanetary magnetic field (IMF) and solar wind plasma. The IMP 8 satellite is located in a nearly equatorial 30- to 40-R_E elliptical orbit and was roughly upstream of the Earth during the 2 days presented here. IMP 8 data used here are hourly averages of plasma parameters and 15-s samples of the magnetic field. We also analyzed Defense Meteorological Satellite Program (DMSP) observations of the location of the auroral precipitation region during these 2 days. The DMSP satellites are in a nearly polar low Earth orbit (~900-km altitude) with a 98° angle of inclination. The boundary plasma determination is made by the DMSP automated boundary identification procedure [*Newell et al.,* 1991].

3.1. Case I: October 3, 1988 (Day 277)

Plate 1 is a spectrogram of the South Pole Station magnetic field and ELF-VLF data from 1000 to 2000 UT. Local magnetic noon for the South Pole occurs at 1530 UT. The spectrograms were produced by performing 256-point fast Fourier transforms on data, which were time differenced in order to flatten the background spectra. The spectral power for each channel is plotted in a separate panel using a logarithmic scale with two color shades per decade. The vertical axis shows the frequency of oscillation from 0 to 500 mHz and is the same for all panels. The top two panels of this figure, XBB and YBB, show search coil magnetometer data and are used to identify ULF magnetic pulsation events, which appear as narrow bands at ~0.03 Hz. The bottom three panels show the modulation spectra of the VLF1, VLF2, and VLF3 signals. Note that the ELF-VLF receiver channel outputs represent the band-pass limited and detected wave power and that the panels in Plate 1 show the ULF amplitude modulation content of this ELF-VLF wave power.

The top two panels of Plate 1 show magnetic pulsations at ~30 mHz that are almost continuous in both the XBB and YBB components for the entire period displayed. The VLF1 channel shows modulation at this same frequency from 1400 to ~1900 UT with the modulation also apparent in the VLF2 channel from 1800 to 1900 UT. The vertical stripes in the spectrogram occurring every 15 min are due to interference from an ionospheric sounder. The relatively broadband intensifications in the VLF1 channel during the early part of the day (1000-1200 UT) represent a general enhancement of wave activity, which may be auroral hiss, polar chorus, or whistlers originating in the

conjugate hemisphere. The nature of the waves cannot be determined, because wideband VLF data from South Pole Station were not available for this period and is not relevant for this study, which focuses on the more narrowband QP emissions. The higher-frequency (~100 mHz) magnetic pulsations later in the day are Pc 1 and Pc 2 emissions, which are also unrelated to the QP observations discussed here.

Figure 1 shows logarithmic power spectra of 2048 one-second samples from these data channels for a 34-min period starting at 1809 UT, a time when the two lower-frequency ELF-VLF channels show some QP modulation at ~30 mHz. The error bar represents the 99% confidence level according to Fisher's test for a 2048-point power spectrum [Fuller, 1976]. The dashed vertical line represents the expected frequency for Doppler-shifted upstream ion cyclotron waves in the IMF based on elementary theory [Gul'elmi, 1974]

$$f \text{ (Hz)} = 0.006 \, |B_{IMF}| \text{ (nT)} \qquad (1)$$

using the 1-hour averaged $|B_{IMF}|$ value measured by IMP 8 for the hour from 1800 to 1900 UT. The broad peaks in both the magnetometer and ELF-VLF channels centered roughly at this frequency suggest that these pulsations may be driven by upstream ion cyclotron waves, consistent with many previous ground-based and satellite observations of Pc 3-4 pulsations [Gul'elmi, 1988; Engebretson et al., 1991; Morrison et al., 1994]. The only other statistically significant peaks in this figure are near 0.15 Hz in the magnetometer channels, corresponding to the Pc 2 emissions so prominent in Plate 1.

Figure 2 shows IMP 8 data for the day shown in Plate 1 as well as the occurrence of the QP observations in the different channels. The panels, from bottom to top, are as follows: solar wind flow speed (kilometers per second), dynamic pressure (nanopascals, assuming a solar wind composition of 96% protons and 4% helium ions), IMF cone angle (degrees, angle between the Earth-Sun line and B_{IMF}), and B_z (nanoteslas, in GSM coordinates). Gaps in the plot indicate intervals when
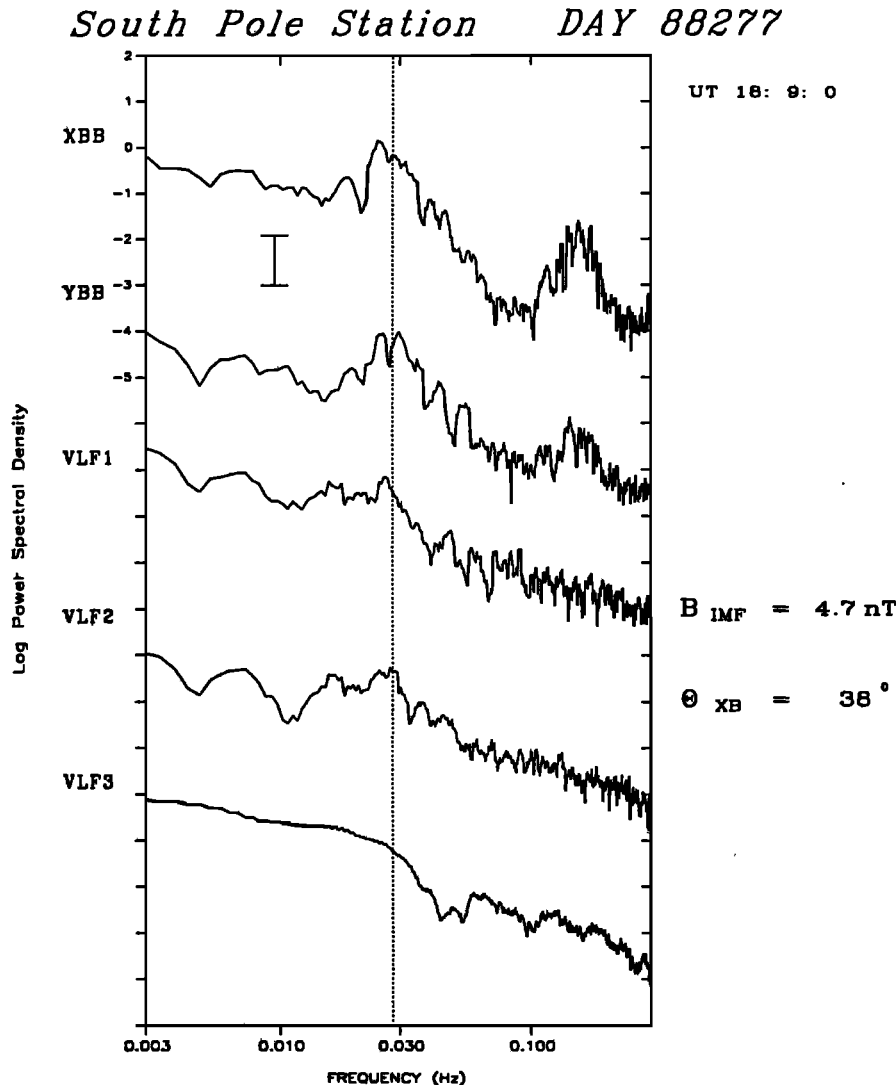

Figure 1. A log-log plot of Fourier spectra of magnetic field and ELF-VLF band-pass receiver data for 1809 to 1843 UT (2048 one-second samples) on October 3, 1988 (day 88277). Traces are in the same order as Plate 1. The error bar represents the 99% confidence level according to Fisher's test for a 2048-point power spectrum. The dashed vertical line represents the expected frequency for Doppler-shifted upstream ion cyclotron waves in the interplanetary magnetic field (IMF) based on elementary theory [Gul'elmi, 1974] and using the averaged IMF magnitude observed between 18:00 and 19:00 UT.
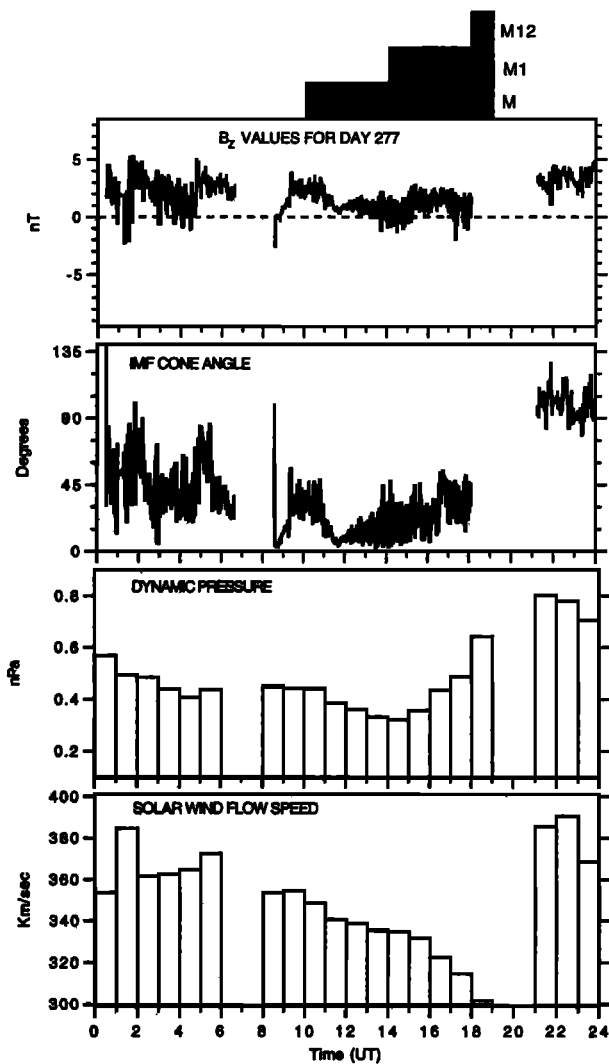
Figure 2. Hourly averaged IMP 8 data for October 3, 1988 (day 88277). From top to bottom the panels are as follows: IMF B_z component (in GSM coordinates, in nanoTesla), IMF cone angle (angle between the Earth-Sun line and B_{IMF}, in degrees), solar wind dynamic pressure (nPa), and solar wind flow speed (km/sec). The occurrence of Pc 3 and QP events in the different frequency channels is indicated above the top panel.

IMP 8 data were not available. The occurrence of QP events in the different frequency channels is indicated at the top of the figure. The M row indicates the period when ~30 mHz magnetic pulsations were observed in either the X or Y component of the magnetometer. The M1 row indicates the period of time when modulation in the VLF1 channel occurred simultaneously with the magnetic pulsations, and M12 indicates periods when both the VLF1 and VLF2 channels showed similar pulsations.

Figure 2 illustrates the dependence on the solar wind activity of the observation of QP events. The IMF B_z component is slightly negative for a brief period shortly before 0900 UT, more than 3 hours before the onset of magnetic pulsation or QP activity, but during the remainder of the interval from 0900 to after 1800 UT the IMF is predominantly radial and on average B_z is positive. It is understood that for upstream waves to effectively couple into the magnetosphere the cone angle must be near 0° or 180° and typically within 45° of these extrema

[*Greenstadt and Russell*, 1994]. Throughout this period the cone angle is favorable for the coupling of upstream waves into the magnetosphere, consistent with the nearly continuous ~30 mHz magnetic pulsations seen in Plate 1. The increase in the cone angle that must have occurred sometime between 1900 and 2100 UT may be responsible for the termination of the QP emissions. As the dynamic pressure increases between 1400 and 1900 UT, we see a transition from M1 to M12 emissions, suggesting that solar wind parameters may play a role in determining the frequency of QP emissions.

Information from the DMSP automated boundary identification data base for this day (not shown) gave evidence that the dayside magnetosphere was apparently expanded on this day, and the polar cap contracted. The DMSP satellite encountered the boundary plasma (BP) region only once on the day side, at 1940 UT, and the poleward boundary of the BP region on the nightside often was observed at large invariant latitudes (>~80°). Because the auroral oval is typically offset from the geomagnetic pole, and is at higher magnetic latitude near noon than near midnight [*Holzworth and Meng*, 1975; *Meng et al.*, 1977], these data suggest a significantly contracted oval. The invariant latitude of the poleward boundary of the BP region did, however, show a steady decrease from 1400 to 2000 UT, indicating that the increasing solar wind dynamic pressure apparently compressed the magnetosphere (and expanded the auroral oval). As the oval expanded, modulated ELF-VLF emissions were seen to expand to higher frequencies.

3.2. Case II: May 10, 1988 (Day 131)

Plate 2 and Figures 3 and 4 use the same format and show the same type of data as Plate 1 and Figures 1 and 2. In Plate 2 the top two panels both show a fairly monochromatic signal having a center frequency of ~30 mHz; it starts near 1000 UT, is strongest from 1320 to 1630 UT, and continues with varying intensity throughout most of the 10-hour period shown. Some broadband magnetic disturbances are also evident, for example, from 1300 to 1320 UT and from 1650 to 1750 UT, as well as some Pc 1 activity before 1200 UT. The ELF-VLF panels show a typical quasi-periodic event also starting at ~1320 UT. It extends to ~1700 UT in VLF1 and VLF2 channels but only to ~1430 UT in the VLF3 channel. Two brief and less intense QP events are evident in the VLF2 channel starting at ~1900 and ~1940 UT. Both of these are accompanied by weak modulations in both magnetometer channels and in the VLF1 and VLF3 channels as well. Figure 3 shows stacked spectra of these data channels at ~1345 UT, a time when all three ELF-VLF channels show the same QP modulation. Only the peak in the VLF2 channel near 42 mHz is statistically significant at the 99% confidence level, but the spectra from all five channels show broad peaks near this same frequency, which, as in Figure 1, matches the frequency predicted from the simultaneous observations of the IMP 8 magnetometer.

Figure 4 shows the available IMP 8 data for this day as well as the occurrence of the QP observations in the different channels. The dynamic pressure starts out on this day at 1.4 nPa but after a data gap is observed to be above 1.7 nPa at 1100 UT. It then falls to a value about 30% lower (1.2 nPa) near 1400 UT and rises again to a second maximum of 1.6 nPa near 1900 UT. The IMF is also considerably more variable on this day, with large fluctuations in cone angle and several excursions of B_z to below -2 nT, for example, from 1150 to 1230, from 1520 to 1600, and near 1720 and 1930 UT. Negative (southward) B_z
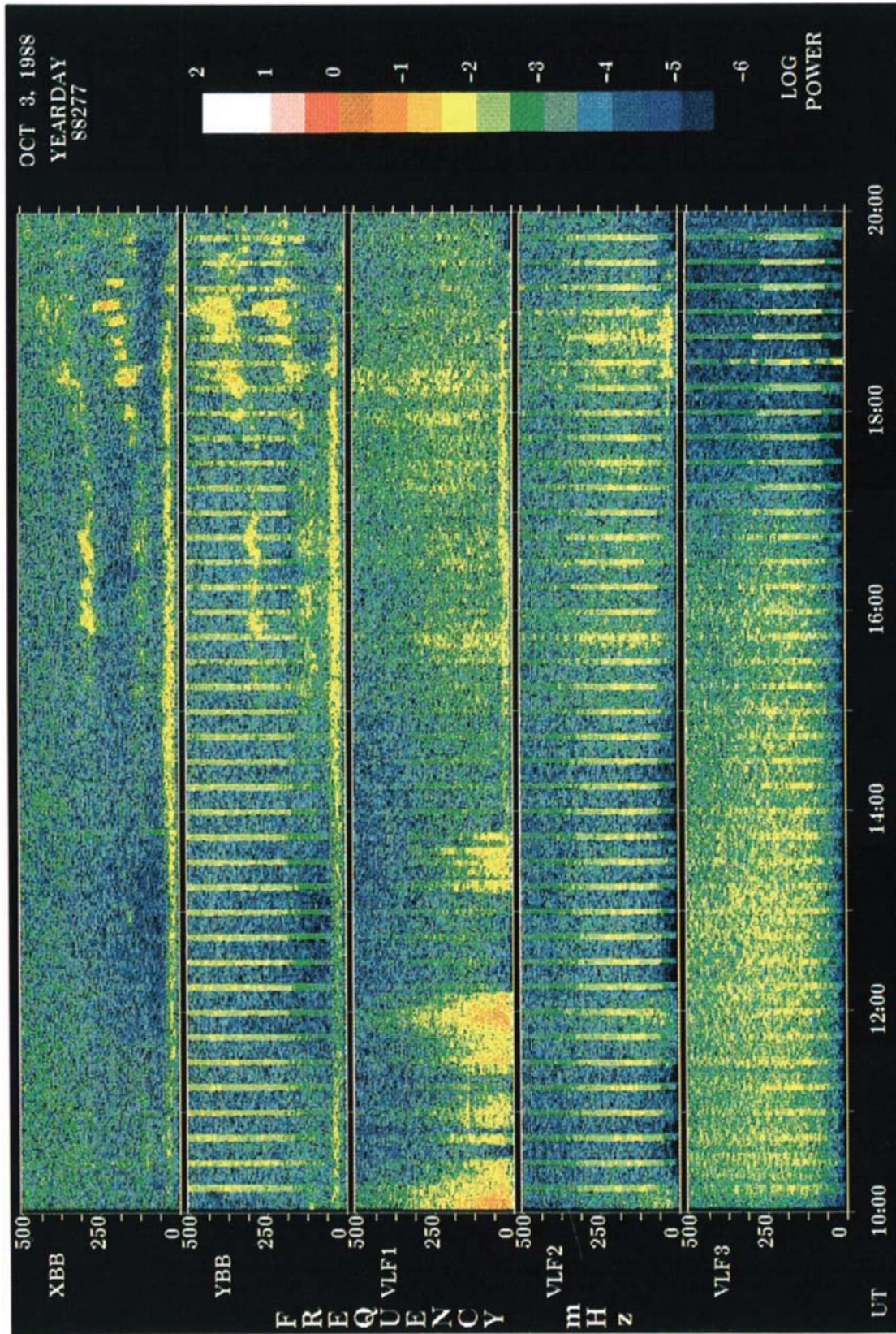
Plate 1. A spectrogram of magnetometer and VLF data from South Pole Station for October 3, 1988 (day 88277). The top two panels are XBB and YBB (N-S and E-W components of the magnetic field) from a search coil magnetometer. The third, fourth, and fifth panels are VLF1 (0.5 to 1.0 kHz), VLF2 (1.0 to 2.0 kHz), and VLF3 (2.0 to 4.0 kHz), respectively.
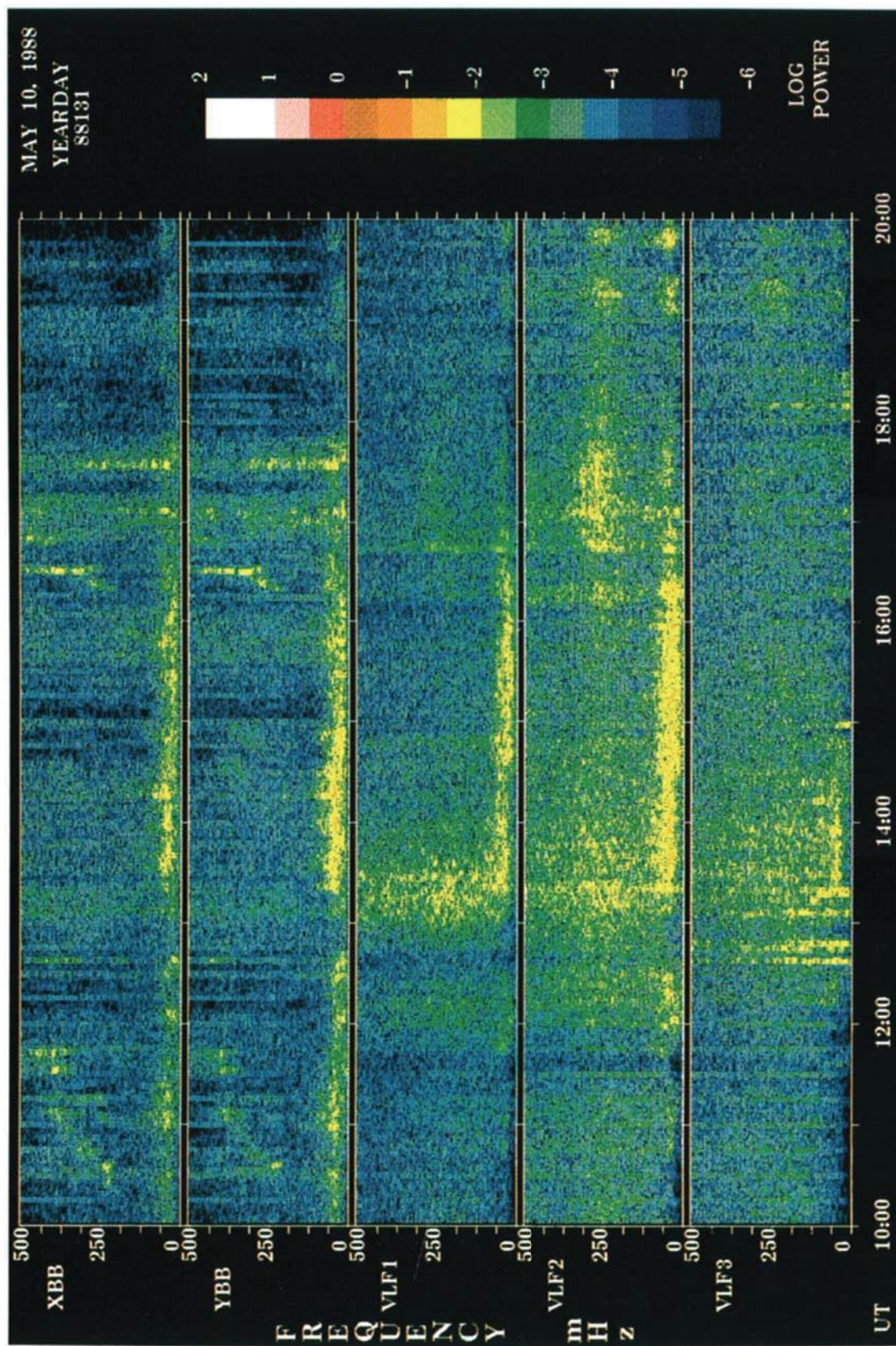
Plate 2. A spectrogram of magnetometer and VLF data from South Pole Station for May 10, 1988 (day 88131), as in Plate 1.
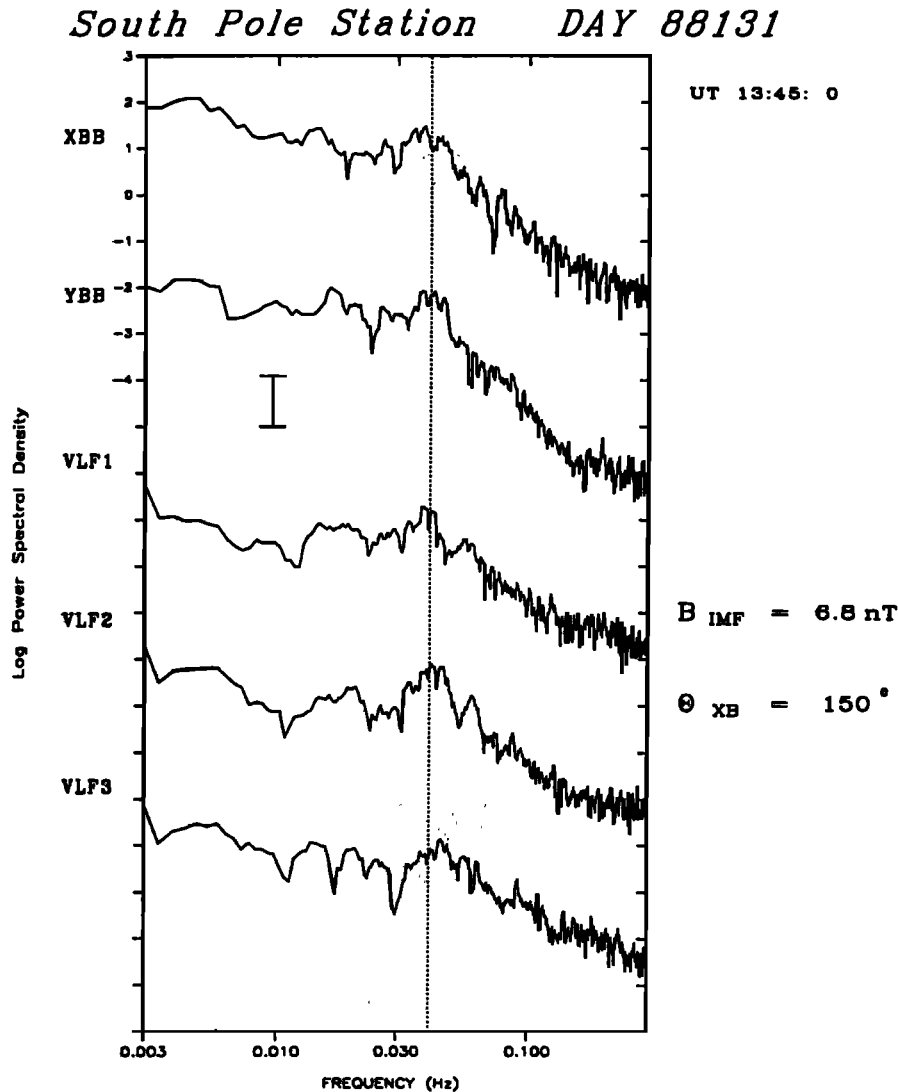
Figure 3. A log-log plot of Fourier spectra of magnetic field and ELF-VLF band-pass data from 1345 to 1419 UT on May 10, 1988 (day 88131), as in Figure 1. The dashed vertical line is the expected frequency for Doppler-shifted upstream ion cyclotron waves using the average IMF magnitude observed between 1300 and 1400 UT.

components are associated with inward movement of the dayside magnetopause, possibly through reconnection [*Roelof and Sibeck*, 1993], and with equatorward movement of the cusp [*Carbary and Meng*, 1986]. Although the dynamic pressure actually decreased slightly at 1300 UT, the southward B_z interval near 1200 UT may contribute to the onset of M123 events observed at 1300 UT and might also contribute to the later onsets with lower amplitude after 1900 UT. The IMF cone angle is well above 135° from 1200 to 1230 UT, from 1325 to 1650 UT, and intermittently after 1800 UT. The solar wind flow speed further illustrates the variability in the solar wind on this day. It is quite clear from this figure that near 1200 UT the solar wind conditions are favorable for both upstream wave coupling and magnetospheric compression, and it is shortly after that time that we observe the QP emissions in all three channels. DMSP boundary identification data indicated a more expanded oval throughout this day, again consistent with the simultaneously observed solar wind conditions.

3.3. Implications

These examples suggest that there may be several factors which affect the frequency and occurrence of QP events. The primary one is the requirement of a source for the magnetic pulsations which drive the type 1 QP emissions. The characteristics of the two cases discussed above are consistent with upstream ion cyclotron waves in the foreshock region being the primary source for two reasons: (1) as noted above, the center frequency of the QP modulations fits the value predicted for upstream waves [*Gul'elmi*, 1974], and (2) the small IMF cone angles observed imply that protons reflected from the bow shock will generate waves in regions that will be convected toward the subsolar bow shock, thus allowing effective coupling into the magnetosphere [*Greenstadt and Russell*, 1994].

The carrier frequency and occurrence of QP events also appear to be linked to the geometry of the magnetosphere. In the two cases shown the QP modulation appears to expand into a
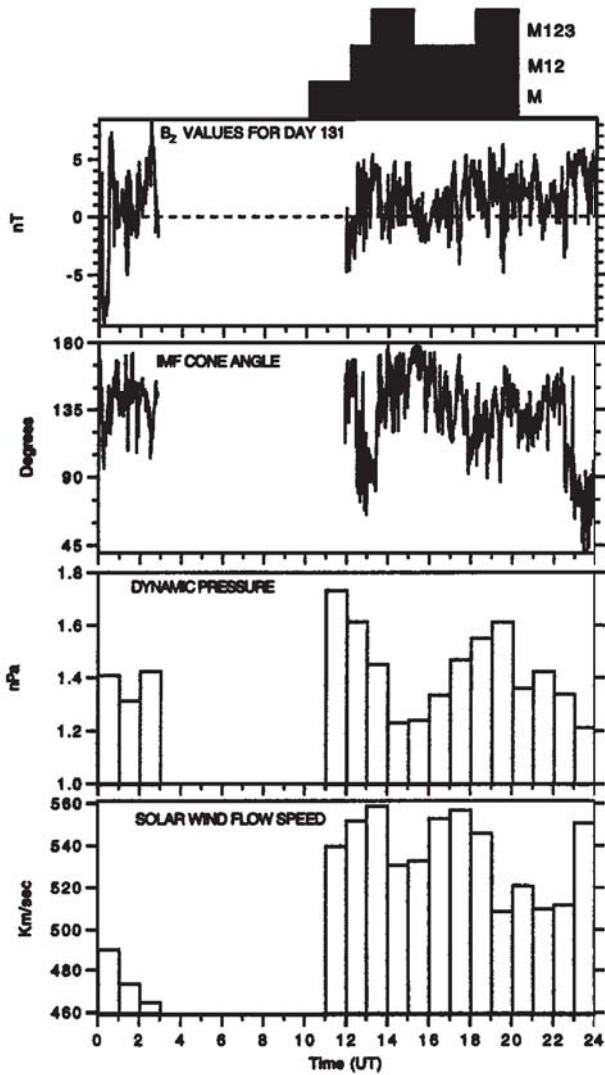
Figure 4. IMP 8 data for May 10, 1988 (day 88131) as in Figure 2.

only one event was counted per hour. For January, April, July, and October of 1988 all 24 hours of each day were surveyed for events. It was soon determined, however, that nearly all of the events were limited to a period between 1000 and 2000 UT, and hence the analysis was limited to that period. Events are identified as M, M1, M12, etc., on the basis of which data channels show the characteristic signature described above. M denotes modulations in just the magnetometer channels (Pc 3 signals almost always appeared simultaneously in both X and Y components), and the numbers denote the ELF-VLF channels which also showed a modulation at roughly the same frequency as the magnetic pulsations.

A study of these daily spectrograms for the 10 months of available data for 1988 (January through October) revealed an increase in the number of M1 (ULF-VLF1) events in the months after June. We subsequently added data to this study from September through December 1987 and found a similarly increased rate of occurrence. Figure 5a illustrates this effect by showing a comparison of monthly totals of M1 and M12 events, denoted by shaded and open bars, respectively. The monthly occurrence totals have been normalized to compensate for those hours when records were missing or unreadable (monthly coverage averaged 78% with a standard deviation of 4%). The combined event count is largest during two 3-month periods, October through December 1987 and July through September 1988, and also exhibits an isolated monthly peak in March 1988.
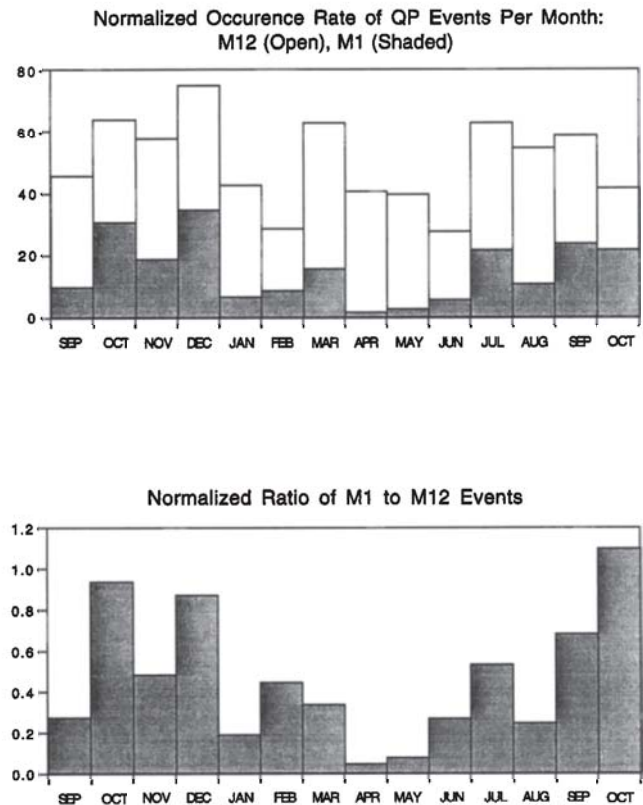

Figure 5. (a) A histogram of the number of M1 and M12 events observed each month in late 1987 and 1988 at South Pole Station. M1 events are indicated by the shaded bars and M12 events are indicated by the open bars. (b) A histogram of the ratio of M1 events to M12 events for each month at South Pole Station.

higher-frequency band at times when either the solar wind dynamic pressure rises or the IMF B_Z component turns southward. Both of these changes are known to compress the dayside magnetosphere (see, for example, Figure 9 of *Roelof and Sibeck* [1993]). To investigate further the causes of QP emissions and to verify the trends discussed above, we performed a statistical study on all QP events observed at South Pole Station during late 1987 and 1988.

4. Statistical Study

To identify all of the QP events during this period, dynamic spectrograms of the magnetometer and ELF-VLF data, such as Plates 1 and 2, were examined for each available day. QP events were identified in hourly intervals by analyzing each of the daily dynamic spectrograms. Each event in the magnetometer and ELF-VLF channels in the spectrograms was required to be (1) band-limited (bandwidth < 100 mHz), (2) centered in the Pc 3 frequency range, between approximately 20 mHz and 60 mHz; and (3) appear at least two color shades (10 dB) above the background. The duration of the emissions also had to be at least 20 min to be counted as an event in a given hourly interval, and

The number of M12 events appears to have roughly equal maxima near all three equinox periods, while the number of M1 events is clearly larger during the fall equinoxes than during spring equinox. Although the M1 event counts show considerable variation from month to month and are somewhat larger in fall 1987 than in fall 1988, Figure 5a suggests the existence of an apparent seasonal variation in the occurrence and frequency of QP events which may provide clues to the location and mechanism of their generation.

Figure 5b illustrates this seasonal variation even more clearly. We have plotted the ratio of M1 events to M12 events for each month. October 1988 is the only month where the number of M1 events exceeds the number of M12 events, but most months near the fall equinox have relatively high ratios as well. We found this variation unusual because it did not show symmetry with respect to the solstices as one might expect, but rather it differentiated between the spring and fall seasons of the year.

To determine the effect of geomagnetic activity on our observations, we calculated the average Kp index during the hours that contained events in each major category. For the entire 14-month data set the average Kp value during M events was 2.09, during M1 events 1.59, during M12 events 1.78, and during the much more infrequent M123 events 2.04. For the 1988 events only, the Kp averages for M events (1.59) and M12 events (1.56) were similar, whereas for M1 events the average was 1.37, and for M123 events the average was 1.79. Although the Kp values for all categories listed are somewhat larger for the 14-month data set than for the 10-month data set in 1988, they retain their relative order, with Kp for M1 $< Kp$ for M12 $< Kp$ for M123. This trend in frequencies is consistent with inferences from the two case studies above. The relatively low Kp levels of all categories are not surprising, both because the requirement for a low IMF cone angle is not particularly favorable for the onset of substorms and because for higher levels of activity the auroral oval will expand equatorward and possibly put cusp-latitude stations such as South Pole out of reach of such emissions [Engebretson et al., 1994].

We also investigated the diurnal variation of the occurrence of each type of event for each month and averaged over the 14 months of available data. The average diurnal variations of the four most commonly occurring event types (M, M1, M12, and M123) are shown in Figure 6. The monthly divisions did not show any significant differences from these totals. For example, M events occurred during 35% of all available hours between 1000 and 2000 UT, with a standard deviation of 5%, while the total of all QP event types occurred during 17% of all available hours, with a standard deviation of 3%. The other event types did not have enough occurrences to be statistically significant (nine M2 events, three M23 events, and one M3 event). There is an interesting trend in that as the frequency increases, the occurrence peak moves to a later time in the day. The M events, which are Pc 3 magnetic pulsations without associated QP emissions, peak at ~1230 UT, 3 hours before local magnetic noon. The M1 events show two peaks, one at ~1300 and another less significant one at ~1630 UT. The M12 events peak at ~1430 UT, only 1 hour before magnetic local noon. The M123 events show the latest peak (~1630 UT) of any event type sampled.

A similar diurnal trend is evident in two other studies at lower L shells. Sato et al. [1990] presented measurements of the signal strength of auroral zone VLF hiss observed at Syowa Station, L=6, as a function of UT. Figure 1 of their paper shows a peak at ~1230 UT (local noon is ~1200 UT) for the 750-Hz
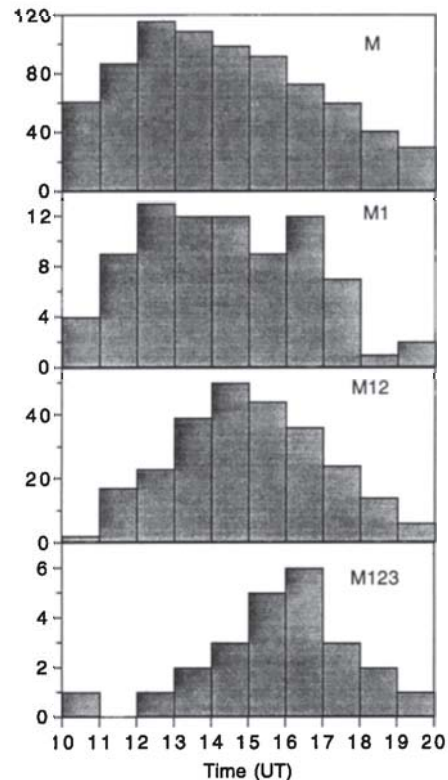

Figure 6. A histogram of occurrences of the four most common QP event types at South Pole Station as a function of universal time.

ELF channel and Figure 3 shows a peak in 2-kHz emissions at 1330 UT. The conjugate station (Husafell) did not show this trend. Morrison and Freeman [1995] presented occurrence distributions of QP events observed at Halley, Antarctica (at L = 4 and, like South Pole, with local magnetic noon ~1530 UT), based on digitally recorded power levels in two ELF-VLF passbands, 0.5-1.5 kHz and 2.5-3.5 kHz. Their Figure 2 shows a diurnal occurrence distribution of QP events in the 0.5-1.5 kHz channel that is quite similar to the M12 events panel in Figure 6 of this study: both have clear peaks slightly before local noon. A possible explanation for these diurnal variations will be presented below.

5. Discussion

In order to establish a context for our discussion we present the following model for the generation of QP emissions. In this model there are two essential criteria for the generation of QP emissions: (1) an intense interaction must occur between electrons and electromagnetic waves, leading to the emission of ELF-VLF chorus and/or hiss, and (2) Pc 3 pulsations must travel through this region to modulate the ELF-VLF emission intensities. Any source region we propose must fulfill these criteria and be capable of generating ELF-VLF waves that propagate to the point of observation (South Pole Station). Because we have limited our discussion to type 1 QP emissions, the Pc 3 waves which generate the QP emissions must also propagate from the source region to the point of observation.

The first-order cyclotron resonance condition, $\omega + (\mathbf{k} \cdot \mathbf{v})_\parallel \approx \Omega^-$, (where ω and $\mathbf{k}$ are the wave frequency and wave number, respectively, $\mathbf{v}$ is the particle velocity, and Ω^- is the local

electron gyrofrequency) can be satisfied by whistler mode waves ($\omega < \Omega^-$) when waves and electrons travel in opposite directions. On closed field lines this condition is usually thought to lead to the most intense emissions near the equator for two reasons. First, because electron densities in the outer magnetosphere typically decrease exponentially with increasing energy, the greatest number of electrons will satisfy the resonance condition for a given wave frequency in regions of minimum B field [see *Tsurutani and Smith*, 1977]. Second, near a field minimum the interaction region between waves and electrons is likely to be relatively homogeneous, thus providing longer wave growth times [*Helliwell*, 1970]. Many aspects of this wave-particle resonant interaction are reviewed by *Inan et al.* [1983].

Using this model as a context, we present here a plausible explanation for the observed seasonal variations and try to identify the source region(s). We start by mapping the magnetic field line connected to South Pole Station at local magnetic noon (1530 UT) using the *Tsyganenko* [1991] field model. Since the Earth's dipole axis tilt changes throughout the year, distortions due to the solar wind change the shape of the geomagnetic field. One effect of these changes is the formation of regions of minimum magnetic field far from the equatorial plane, which we denote as the northern and southern "horns". *Morrison et al.* [1994] have argued that QP modulation should be highly efficient in these minimum-field regions located near the exterior cusp, and we also expect that these local regions of slowly varying magnetic field will be favorable to wave-particle interactions and wave growth. The magnetic field geometry also affects the propagation of the ELF-VLF waves from the source region along the magnetic field lines. Because ELF-VLF waves cannot propagate at frequencies higher than one-half of the local electron cyclotron frequency, because of ducting requirements [*Helliwell*, 1965], a minimum in the magnetic field magnitude acts as a barrier for waves that have frequencies larger than half the lowest cyclotron frequency.

Figure 7 is a plot of the minimum magnetic field values at local magnetic noon along the field line that maps to South Pole Station throughout the year based on the *Tsyganenko* [1991] field model for $Kp = 2$. This choice of Kp value is justified by considering the average Kp indices for the event categories discussed above. The plot shows the northern and southern minima (horns) as well as the equatorial magnitude of the South Pole field line plotted for the 21st day of each month. This summary of the magnetic field model indicates a striking asymmetry: there is little variation in the equatorial and northern horn magnetic field values throughout the year, but there is a significant decrease from January to June in the southern horn region values. The asymmetry, caused by the large offset between the geographic and magnetic poles in the southern hemisphere, is largest at this magnetic longitude. This decrease in southern horn field strength should have two effects on our observations: (1) it should increase the total number and/or intensity of QP events, because deeper minima would be more sensitive to variations in total field [*Morrison et al.*, 1994], and (2) it should decrease the ELF-VLF frequency of the QP events, because the higher frequencies are either not produced or cannot propagate to the ground. The labeled values of the electron cyclotron frequency (F_{ce}) in Figure 7 demonstrate most clearly the second effect. If the outermost field line has a small cyclotron frequency (< 1 kHz) in the southern horn region, then QP modulation in this region should be most efficient at much smaller frequencies, and the field line minimum will block any QP emissions from the equatorial region or the northern horn region. During such times we could only observe QP variations in the VLF1 channel (0.5-1 kHz). Values given in the figure for F_{ce} at the southern horn minimum are in rough quantitative agreement with the frequency variations we observed. (Readers should note, however, that the *Tsyganenko* [1991] model is of limited validity very close to the magnetospheric boundary [*Stern and Tsyganenko*, 1992].)
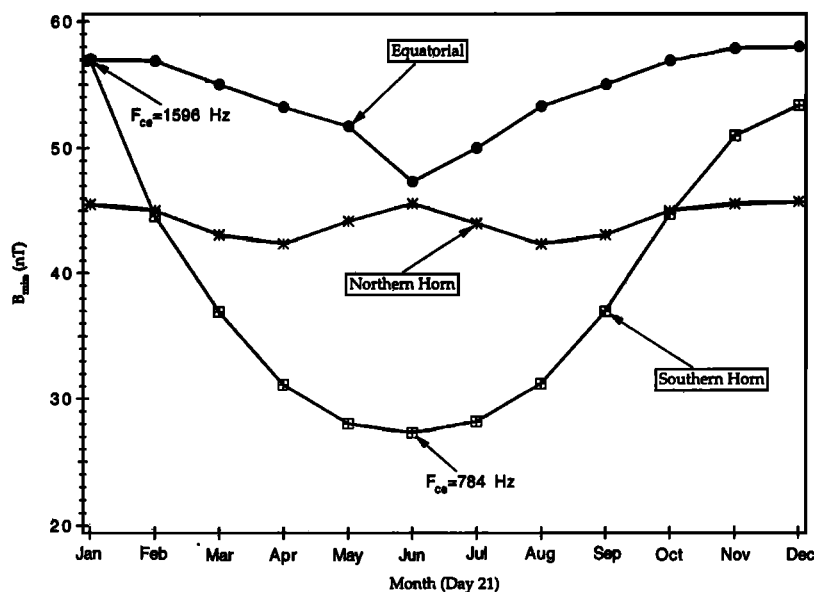

Figure 7. A plot of the minima based on the *Tsyganenko* [1991] model of the geomagnetic field for the field line starting at South Pole Station, calculated for the 21st of each month at 1530 UT (local magnetic noon). The equatorial value was determined by using the low-latitude field lines to determine the magnetic equatorial plane. This was extended out to the South Pole line to determine the location of the equatorial region for that line.

The formation of horn regions implies that more M1 events should be observed at southern hemisphere ground observatories when the southern horn is most prominent (assuming, of course, that trapped electron populations, presumably injected on the night side, do not change substantially). Although the *Tsyganenko* [1991] field model predicts this effect should be most prominent in June, the maximum occurrence of M1 events in our data set is about 3 months later, near fall (but not spring) equinox (see Figure 5). One significant reason for this discrepancy may be that the *Tsyganenko* [1991] empirical model does not take into account the IMF orientation or magnitude; it includes diurnal and dipole tilt effects, but geomagnetic activity is parameterized using only *Kp*.

The seasonally varying interaction between the Earth's magnetic field and the IMF, referred to as the Russell-McPherron effect and known to influence the probability of geomagnetic storm occurrence, may also be relevant to variations in QP occurrence probability. *Russell and McPherron* [1973] studied the orientation of the IMF as viewed from a geostationary coordinate system and considered the importance of geometrical effects governing the interaction between the IMF and the magnetospheric field on the observed seasonal variation in substorm occurrence. In particular, they determined the intrinsic southward (and northward) extent of a purely ecliptic "garden hose" IMF due to the tilt of the Earth's dipole axis. The contour plots shown in Figures 8 and 9 (Figures 5 and 9 in their original paper) show the maximum southward IMF component (B_z) as a function of month and universal time in two coordinate systems. The B_z value in GSM coordinates, plotted in Figure 8, shows two nearly equal maxima for 1530 UT (local magnetic noon for South Pole), one in early April and the second in early October. *Russell and McPherron* [1973] found that these maxima matched the dates of the observed statistical maxima of substorm occurrence.

The contour plot in Figure 9 is similar to that of Figure 8, but it uses the SM coordinate system with z component parallel to the Earth's dipole axis. *Russell and McPherron* [1973] noted that this coordinate system may be more applicable to high-

latitude processes, because it intrinsically includes the tilt of the dipole axis away from and toward the sun. This plot shows maxima in the southward component of the IMF occurring in mid-August and February, with the August maximum a factor of 3 larger and with the local time of deepest (negative) maximum shifted in local time to ~1400 UT, nearer the time of magnetic local noon at South Pole Station. *Russell and McPherron* [1973] were only interested in the southward excursions of the IMF and therefore set all northward components to zero. For our study the northward excursions appear to be more important. Because of the toward/away symmetry of the IMF, a plot using a reversed IMF direction would yield the same contour plot with positive values replacing the negative values. The periods of extreme northward IMF are important to the study of quasi-periodic events because the dayside magnetosphere will tend to expand during such times and the horns will form at higher latitudes, thus having lower minimum fields. Unfortunately, we know of no quantitative magnetic field model that combines the seasonal tilt and variation in IMF direction in a unified manner.

We interpret the seasonal variations of QP occurrence and frequency observed in South Pole data as being intrinsically related to the solar wind - magnetosphere interactions modeled by *Russell and McPherron* [1973] because of the offset of the SM and GSE coordinate systems. For the same range of low IMF cone angles associated with the presence of upstream waves near the subsolar bow shock the dayside magnetosphere will be on average more expanded, and the southern hemisphere horn will have a deeper minimum, near fall equinox than at other times of the year, because of the more positive B_z component of the IMF expected on average during this season. Figure 10 shows in schematic form the influence of the IMF in this model. Even without any change in the shape of the dayside magnetopause, the latitudinal movement of the cusps associated with changes in IMF B_z will cause significant changes in the curvature and field magnitude of the horn regions, with a weaker field for $B_z > 0$ (Figure 10a) than for $B_z < 0$ (Figure 10b). The weaker horn field configuration for $B_z > 0$ should increase the likeli-
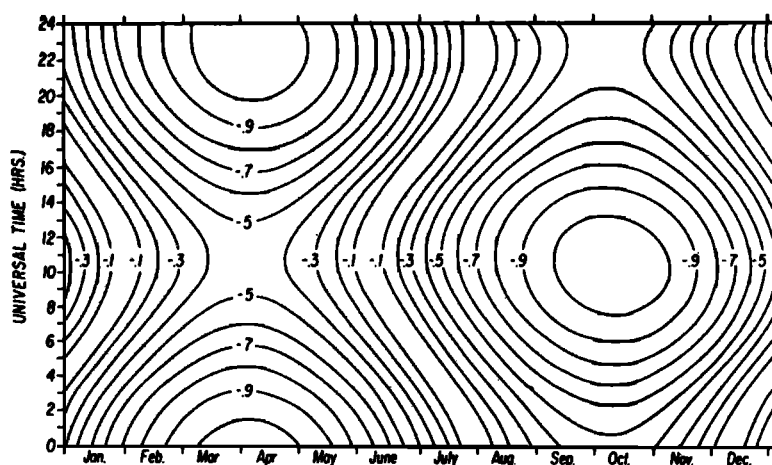

Figure 8. Reprint of Figure 5, including caption, from *Russell and McPherron* [1973]. "A contour plot in gammas (nT) of the diurnal and annual variation of the effective average southward component in the GSM system due to inward and outward fields of 5 γ along the ideal interplanetary spiral in the GSEQ system. The solar equatorial longitude of the spiral field has been taken to be $135°$ and $315°$. Northward components were set to zero in the average. The more negative the contour the more geomagnetically active the interval should be on the average."
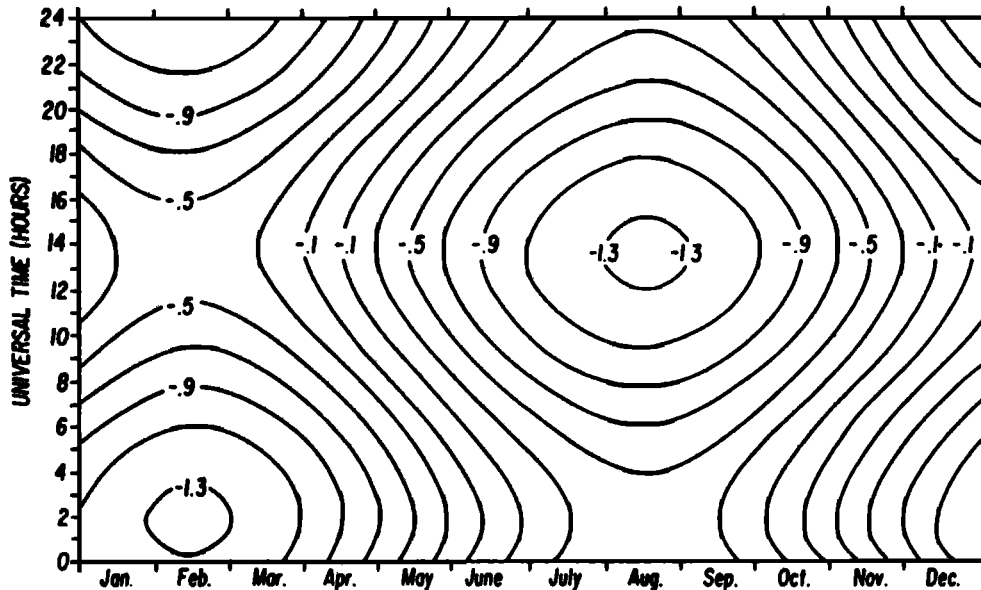
Figure 9. Reprint of Figure 9, including caption, from *Russell and McPherron* [1973]. "A contour plot in gammas of the diurnal and annual variation of the effective average southward component in the solar magnetic coordinate system. The interplanetary field and same interaction as used in Figure 5 have been used in constructing these contours."

hood of efficient modulations of wave-particle interactions in the outer magnetosphere near the cusp region in the presence of Pc 3 waves.

Figure 11 illustrates the generation mechanism that we propose. Upstream Pc 3 waves in the solar wind penetrate both equatorial and southern high-latitude horn regions, but they may be able to more strongly modulate the ELF-VLF hiss produced by trapped electrons in the horn region because of its lower total field. *Morrison et al.* [1994] and *Morrison and Freeman* [1995] clarify the role of upstream waves in this model and provide further evidence in support of this mechanism. The frequency of the ELF-VLF emissions may extend up to one-half of the local electron cyclotron frequency ($F_{ce}/2$); however, the peak emission frequency is expected to be $F_{ce}/4$ [*Tsurutani and Smith*, 1977]. Waves with a frequency greater than half the minimum F_{ce} along a given field line cannot be guided along the field lines and thus will not be observed on the ground. If the source region is on the equatorial side of the southern horn minimum, propagation through the horn region will subject the ELF-VLF emissions to a sharp low-pass filter with a cutoff at half the minimum cyclotron frequency, as is illustrated in Figure

11. Alternatively, if the source region is itself in the horn regions, the resulting ELF-VLF emissions will intrinsically have low frequencies. In either case, whether the waves are generated near the equator or in the horns, the waves observed on the ground at South Pole Station will have only low frequencies. Because the magnetic field varies much more rapidly on the poleward side of the minimum, we do not expect emissions from a region significantly poleward of the horn region.

On more active days the magnetic field in the horn regions will be larger because of magnetospheric compression and/or dayside flux erosion due to reconnection. ELF-VLF emissions on such days will be observed at higher frequencies, because the cyclotron frequency will be higher in the source region (either near the equator or in the horns), and the emissions from the equatorial side of the source region will not be filtered as strongly. This will result in QP emissions appearing in higher-frequency ELF-VLF channels and probably in relatively fewer QP events.

We remind readers that because the variations in observed QP frequency predicted by this model are dependent on asymmetries in the outer dayside magnetosphere caused by offsets
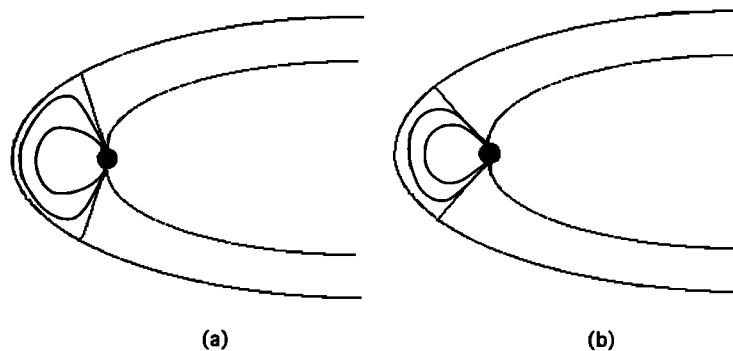

(a)   (b)

Figure 10. A schematic drawing of the Earth's magnetosphere as viewed from the dusk meridian, showing the variation of cusp latitude with IMF B_z: (a) northward B_z, and (b) southward B_z.
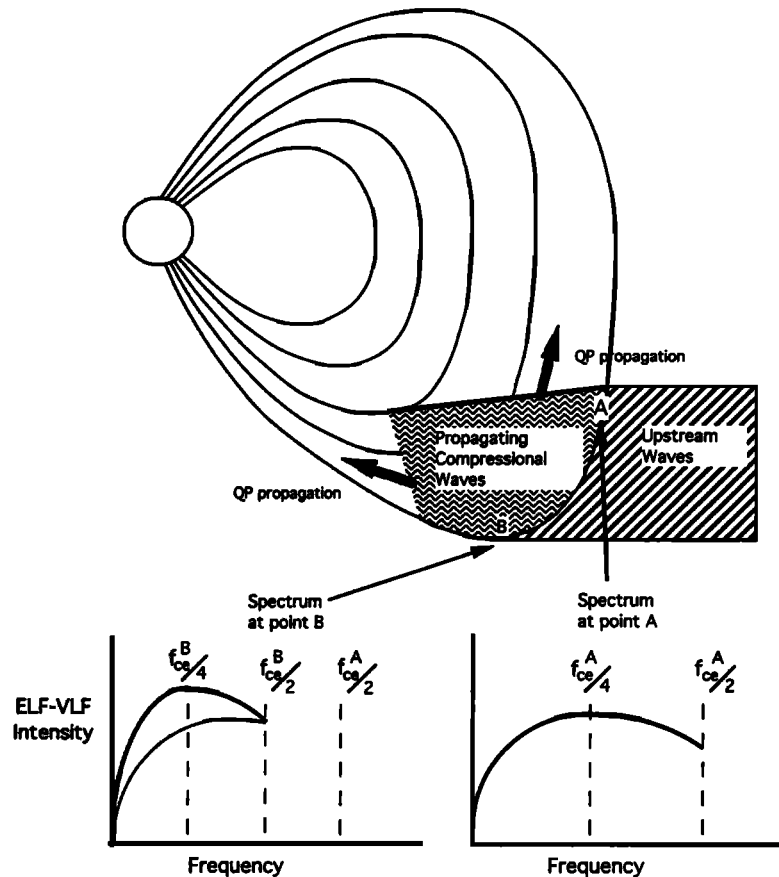
Figure 11. A schematic depiction of the proposed mechanism and source region for the generation of type 1 quasi-periodic ELF-VLF emissions observed on the ground at high southern latitudes. (top) A cartoon depiction of the dayside magnetosphere at local magnetic noon, based on the Tsyganenko [1991] model, showing the southern horn region, which is the region of minimum magnetic field magnitude outlined using a wavy fill pattern. (bottom) The predicted emission spectrum for the ELF-VLF emissions is shown schematically with a bold line at two locations in the top panel, (A) equatorward of the southern horn and (B) in the southern horn region. The thin line in the left hand panel depicts the emissions generated at (A) after being subjected to the low-pass filter as they go through the horn region toward the southern ionosphere.

between the geographic and magnetic poles, this generation mechanism should also result in a somewhat weaker annual variation in QP frequency in the northern hemisphere, with maximum near spring equinox, at the magnetic longitude / universal time at which the north magnetic pole is tailward of the north geographic pole. Simultaneous observations from the northern hemisphere footpoint of the South Pole field line might also help distinguish between the two QP source regions considered here: if QP emissions are generated in the southern horn, the same frequency variation should be detected in both hemispheres. If instead the emissions are generated near the equator and the horn serves primarily as a low-pass filter for ELF-VLF emissions, then QP emissions would be expected to have higher maximum frequencies in the northern hemisphere.

This model of QP production in the horn regions may also be consistent with the observed diurnal variation. We will now speculate on a scenario that may explain the apparent shift in the peak of the diurnal occurrence for the higher-frequency QP events (M12 and M123). If we assume the horn regions are being populated with electrons convecting around the dawn side from the tail region and the minima in the horn regions are sufficiently deep, these convecting electrons will bifurcate into

the weak fields of the northern and southern horn region where they may more easily be scattered into the loss cone near or before local noon. However, in a more compressed magnetosphere a greater fraction of convecting electrons may travel across local noon to reach the afternoon sector before being scattered into the loss cone. Therefore, in a statistical study one might expect the higher frequency events to occur more often in the afternoon and the lower frequency events (indicating a quiet magnetosphere) in the morning, as our data presented in Figure 6 illustrate.

Other observations noted in the statistical study of QP events by Morrison and Freeman [1995] provide some support for this scenario. On the basis of simultaneous broadband data available for several QP events they interpreted the statistically observed drop in the number of events in the higher-frequency channel close to the near-noon peak in the lower-frequency channel as indicative of a change to lower emission frequencies over the noon period and argued that this was additional evidence for a QP emission source in a high-latitude field minimum region.

In our model, geomagnetic activity plays a key role in determining the occurrence and the characteristics of QP emis-

sions. Quiet periods should preferentially produce QP emissions in the lower frequencies. During active periods the horn regions of the magnetosphere should either be stripped away or compressed to higher field levels, and thus high frequency emissions will be observed more frequently. The observed average Kp indices support this assertion, to some extent, in that the M12 and M123 events seem to occur during slightly more active periods. *Tsurutani and Smith* [1977] also noted that the high-latitude, low-frequency chorus events they observed on the dayside with the OGO 5 satellite occurred typically during times of northward IMF B_z and were thus associated with an extended magnetosphere. *Sato et al.* [1990] show a similar effect in Figure 8 of their paper, which shows frequency of occurrence as a function of universal time and Kp for all three frequency bands (750 Hz, 2 kHz, and 4 kHz). The 2-kHz channel for both stations shows more events having higher (>4) Kp values compared to the 750-Hz channel. The only geomagnetically quiet period ($Kp < 2$) showing a significant number of 2-kHz emissions was 2 or more hours after local magnetic noon for the southern hemisphere station. The 4-kHz channel at either station observed a significant number of VLF emissions only at times when Kp was $\sim$ 6.

6. Conclusions

The seasonal variation in the occurrence and characteristics of type 1 quasi-periodic ELF-VLF emissions, which have an occurrence rate of ~17% within several hours of magnetic noon at South Pole Station, Antarctica, may provide important clues to their generation mechanism and source region. Our data show clearly that the low-frequency events (M1) make up a greater percentage of the QP events in the months near fall equinox. Our proposed horn generation mechanism, using only the *Tsyganenko* [1991] field model, predicts that M1 events should occur most frequently around the winter solstice (June 21) because the tilt of the magnetosphere at that time gives rise to the most prominent southern horn region. Inclusion of the interaction between the IMF and the magnetospheric field in a manner analogous to that used by *Russell and McPherron* [1973] leads to good qualitative agreement with our observations and lends additional support to the assertion that QP emissions can be produced in the horn regions. Future study of QP events using data from the newly installed automatic geophysical observatories at several Antarctic sites, along with more continual monitoring of solar wind conditions and in situ observations of the configuration of the high-latitude outer magnetosphere from satellites such as the forthcoming Cluster mission, will be needed to confirm these observations and the physical mechanism proposed here. Regardless of the physical mechanism, the concept of using ELF-VLF signals as ground-based diagnostics of the configuration and dynamics of the outermost magnetosphere deserves additional attention in the coming years.

References

Carbary, J. F., and C. I. Meng, Correlation of cusp latitude with B_z and AE (12) using nearly one year's data, *J. Geophys. Res., 91*, 10047, 1986.

Carson, W. B., J. A. Koch, J. H. Pope, and R. M. Gallet, Long period low frequency emission pulsations, *J. Geophys. Res., 70*, 429, 1965.

Coroniti, F. V., and C. F. Kennel, Electron precipitation pulsations, *J. Geophys. Res., 75*, 1279, 1970.

Engebretson, M. J., B. J. Anderson, L. J. Cahill Jr., R. L. Arnoldy, T. J. Rosenberg, D. L. Carpenter, W. B. Gail, and R. H. Eather, Ionospheric signatures of cusp latitude Pc 3 pulsations, *J. Geophys. Res., 95*, 2447, 1990.

Engebretson, M. J., L. J. Cahill Jr., R. L. Arnoldy, B. J. Anderson, T. J. Rosenberg, D. L. Carpenter, U. S. Inan, and R. H. Eather, The role of the ionosphere in coupling upstream ULF wave power into the dayside magnetosphere, *J. Geophys. Res., 96*, 1527, 1991.

Engebretson, M. J., J. R. Beck, R. L. Rairden, S. B. Mende, R. L. Arnoldy, L. J. Cahill Jr., and T. J. Rosenberg, Studies of the occurrence and properties of Pc 3-4 magnetic and auroral pulsations at South Pole, Antarctica, in *Solar Wind Sources of Magnetospheric Ultra-Low-Frequency Waves, Geophys. Monogr. Ser.*, vol. 81, edited by M. J. Engebretson, K. Takahashi, and M. Scholer, p. 345, AGU, Washington, D.C., 1994.

Fuller, W. A., *Introduction to Statistical Time Series*, 283 pp., John Wiley, New York, 1976.

Greenstadt, E. W., and C. T. Russell, Stimulation of exogenic, daytime geomagnetic pulsations: A global perspective, in *Solar Wind Sources of Magnetospheric Ultra-Low-Frequency Waves, Geophys. Monogr. Ser.*, vol. 81, edited by M. J. Engebretson, K. Takahashi, and M. Scholer, p. 13, AGU, Washington, D.C. 1994.

Gul'elmi, A. V., Diagnostics of the magnetosphere and interplanetary medium by means of pulsations, *Space Sci. Rev., 16*, 331, 1974.

Gul'elmi, A. V., The coefficient of correlation between the frequency Pc 3 and the magnitude of the interplanetary magnetic field (in Russian), *Geomagn. Aeron., 27*(3), 465, 1988.

Haugstad, B. S., Upper cut-off frequency changes in quasi-periodic VLF emission events, *J. Atmos. Terr. Phys., 38*, 781, 1976.

Helliwell, R. A., *Whistlers and Related Ionospheric Phenomena*, p. 5, Stanford Univ. Press, Stanford, Calif., 1965.

Helliwell, R. A., Intensity of discrete VLF emissions, in *Particles and Fields in the Magnetosphere*, edited by B. M. McCormac, p. 282, D. Reidel, Norwell, Mass., 1970.

Ho, D., Interaction between whistlers and quasi-periodic VLF emissions, *J. Geophys. Res., 78*, 7347, 1973.

Holzworth, R. H., and C.-I. Meng, Mathematical representation of the auroral oval, *Geophys. Res. Lett., 2*, 377, 1975.

Inan, U. S., R. A. Helliwell, and W. S. Kurth, Terrestrial versus Jovian VLF chorus: A comparative study, *J. Geophys. Res., 88*, 6171, 1983.

Kitamura, T., J. A. Jacobs, and T. Watanabe, An investigation of quasi-periodic VLF emissions, *J. Geophys. Res., 74*, 5652, 1969.

Lanzerotti, L. J., C. G. Maclennan, L. V. Medford, and D. L. Carpenter, Study of a QP/GP event at very high latitudes, *J. Geophys. Res., 91*, 375, 1986.

Meng, C.-I., R. H. Holzworth, and S.-I. Akasofu, Auroral circle—Delineating the poleward boundary of the quiet auroral belt, *J. Geophys. Res., 82*, 164, 1977.

Morrison, K., and M. P. Freeman, The role of upstream ULF waves in the generation of quasi-periodic ELF-VLF emissions, *Ann. Geophys.*, in press, 1995.

Morrison, K., M. J. Engebretson, J. R. Beck, J. E. Johnson, R. L. Arnoldy, L. J. Cahill Jr., D. L. Carpenter, and M. Gallani, A study of quasi-periodic ELF-VLF emissions at three Antarctic stations: Evidence for off-equatorial generation?, *Ann. Geophys.*, *12*, 139, 1994.

Newell, P. T., S. Wing, C.-I., Meng, and V. Sigillito, The auroral oval position, structure, and intensity of precipitation from 1984 onward: An automated on-line data base, *J. Geophys. Res.*, *96*, 5877, 1991.

Roelof, E. C., and D. G. Sibeck, Magnetopause shape as a bivariate function of interplanetary magnetic field B_z and solar wind dynamic pressure, *J. Geophys. Res.*, *98*, 21421, 1993.

Russell, C. T., and R. L. McPherron, Semiannual variation of geomagnetic activity, *J. Geophys. Res.*, *78*, 92, 1973.

Sato, N., and H. Fukunishi, Interaction between ELF-VLF emissions and magnetic pulsations: Classification of quasi-periodic ELF-VLF emissions based on frequency-time spectra, *J. Geophys. Res.*, *86*, 19, 1981.

Sato, N., and S. Kokubun, Interaction between ELF-VLF emissions and magnetic pulsations: Regular period ELF-VLF pulsations and their geomagnetic conjugacy, *J. Geophys. Res.*, *86*, 9, 1981.

Sato, N., H. Suzuki, and T. Saemundsson, Conjugacy of daytime ELF-VLF emission activities in the auroral zones, *J. Geophys. Res.*, *95*, 7847, 1990.

Stern, D. P., and N. A. Tsyganenko, Uses and limitations of the Tsyganenko magnetic field models, *Eos Trans. AGU*, *73*, 489, 1992.

Taylor, W. W. L., B. K. Parady, P. B. Lewis, R. L. Arnoldy, and L. J. Cahill Jr., Initial results from the search coil magnetometer at Siple, Antarctica, *J. Geophys. Res.*, *80*, 4762, 1975.

Tixier, M., and N. Cornilleau-Wehrlin, How are the VLF quasi-periodic emissions controlled by harmonics of field line oscillations? The results of a comparison between ground and Geos satellites measurements, *J. Geophys. Res.*, *91*, 6899, 1986.

Tsurutani, B. T., and E. J. Smith, Two types of magnetospheric ELF chorus and their substorm dependences, *J. Geophys. Res.*, *82*, 5112, 1977.

Tsyganenko, N. A., Methods for quantitative modeling of the magnetic field from Birkeland currents, *Planet. Space Sci.*, *39*, 641, 1991.

J. L. Alford and M. J. Engebretson, Department of Physics, Augsburg College, 2211 Riverside Ave., Minneapolis, MN 55454. (e-mail: alford@auggie.dnet.nasa.gov; engebrets@augsburg.edu)

R. L. Arnoldy, Science and Engineering Research Building, University of New Hampshire, Durham, NH 03824. (e-mail: Roger.Arnoldy@unh.edu).

U. S. Inan, STAR Laboratory, 321 Durand Building, Stanford University, Stanford, CA 94305. (e-mail: inan@nova.stanford.edu).